

1 HIGH VOLTAGE PULSES CIRCUIT FOR GENERATING A PLASMA PLUME  
2 AT ATMOSPHERIC PRESSURE

3 O. S. STOICAN<sup>1</sup>

4 <sup>1</sup>National Institute for Laser, Plasma and Radiation Physics  
5 Măgurele-Bucharest, Romania  
6 *Email: stoican@infim.ro*

7 *Compiled May 15, 2018*

8 Study of an atmospheric pressure plasma generator driven by a particular elec-  
9 trical circuit is presented. Electrical circuit consists of a high voltage pulses generator  
10 and a common dc high voltage source, parallel connected. The present work was fo-  
11 cused to the enhancement of the high voltage pulses production. A method to optimize  
12 its operation has been devised.

13 *PACS: 52.50.Dg, 52.75.-d, 52.80.Mg, 84.30.-r*

## 14 1. INTRODUCTION

15 Cold plasmas generated at atmospheric pressure comprise a broad range of ap-  
16 plications due to the possibility to process thermally sensitive materials (e. g. [1–7]).  
17 Plasma generator considered here is equipped with an electrical supply block consist-  
18 ing of two voltage sources parallel connected. One of them is a circuit that produces  
19 a train of negative high voltage pulses with peak value of about -4kV, whereas the  
20 other is a conventional dc voltage source whose output voltage can be varied in the  
21 range from -400 V to -1000 V. The purpose of this approach, whose principle has  
22 been previously described in [8], is to avoid the complexity of the classical solutions  
23 based on kilovolts dc sources, rf or microwave fields (e. g. [9–13]). The present work  
24 was focused to the improvement of the high voltage pulses source and its operation  
regime.

## 25 2. EXPERIMENTAL SETUP

26 The block diagram of the experimental setup is shown in Fig. 1. The two elec-  
27 trical voltage sources parallel connected are the high voltage pulses generator HVPG  
28 which ignites periodically the electrical discharge and the dc high voltage source  
29 HVDC which sustains the electrical discharge, respectively. Operating principle,  
30 is based on the well known peculiarity of an electrical discharge in gases, namely  
31 that, the voltage necessary to maintain it is lower than the voltage required to ignite  
it [14]. A diode network consisting of diodes  $D_1$  and  $D_2$  composes the two voltages.

32 Resulting voltage is applied to the cathode K of the plasma source. An unit Spellman  
 33 SL150 was used as dc high voltage source. This equipment allows to vary output  
 34 voltage in a wide range and has as built in available function, the limitation of the  
 35 output current  $I_{dc}$  at a preset value. Supplementary, a ballast resistor  $R_b$  was inserted  
 36 into dc electrical circuit, which was used both as current limiter and current sensor.  
 High voltage pulse generator HVPG, comprising driver Dr, power MOSFET transis-

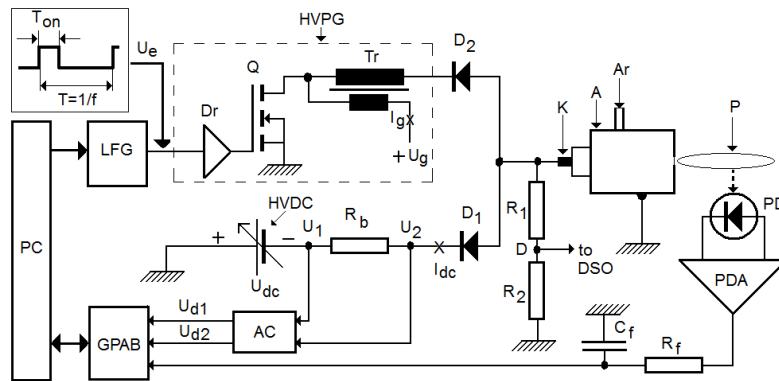


Fig. 1 – Block diagram of the experimental setup. A-anode; K-cathode; P-plasma plume;  $R_1/R_2$  voltage divider; DSO- digital oscilloscope;  $D_1, D_2$ -high voltage rectifiers;  $R_b$ -ballast resistor, HVDC-negative high voltage source; LFG-low frequency signal generator; PD-photodiode; PDA-photodiode amplifier;  $R_f/C_f$ -low pass filter cell; AC-adapter circuit; GPAB-general purpose acquisition board; PC-personal computer. HVPG (dotted rectangle) is high voltage pulses generator consisting of driver Dr, power MOSFET transistor Q and high voltage pulse transformer Tr.

37  
 38 tor Q and high voltage pulse transformer Tr (dotted rectangle in Fig.1), operates as  
 39 a flyback converter. In this way, high voltage pulses can be obtained for a relative  
 40 low transformation ratio [15, 16], this feature representing the main advantage of the  
 41 flyback topology considered for this application. The transistor Q (IRF 840 [17]) is  
 42 driven by the square wave excitation voltage  $U_e$ , with frequency  $f$  and pulse length  
 43  $T_{on}$ , provided by the low frequency signal generator (LFG). The frequency  $f$  can be  
 44 varied in the range from 0.1Hz to 100Hz whereas pulse length  $T_{on}$  has been kept  
 45 constant at 1ms. As a result of current switching through step-up transformer Tr  
 46 primary coil, performed periodically by transistor Q, a train of high voltage pulses  
 47 occurs across its secondary coil. A voltage divider composed of resistors  $R_1$  and  $R_2$   
 48 (voltage ratio  $\simeq 0.15 \times 10^{-3}$ ) allows to display by means of a digital oscilloscope  
 49 connected to point D, the waveform of the voltage applied to cathode K. In Fig. 2 is  
 50 shown the waveform of a high voltage pulse (bottom trace) and its correlation with  
 51 excitation voltage  $U_e$  (top trace). Each sudden current interruption through primary  
 52 coil of the transformer Tr, triggered by falling edge of the excitation voltage, gener-

53 ates a negative high voltage pulse. The circuit is supplied by a dc source delivering  
 54 the voltage  $U_g$  which can be varied in a range from 0V to 5V. Theoretically, the pulses  
 55 voltage peak value increases with increasing of the parameters  $U_g$  or  $T_{on}$ . Due to the  
 56 limitations related to the transformer Tr core magnetic properties, the pulses voltage  
 57 peak was modified only by varying the voltage  $U_g$ , pulse length  $T_{on}$  remaining fixed.  
 58 Diode  $D_2$  rectifies the high voltage pulses occurring at the secondary coil terminals  
 59 of transformer Tr blocking the positive polarity of the pulses. Diode  $D_1$  blocks the  
 60 high voltages pulses to be applied to the dc high voltage output.

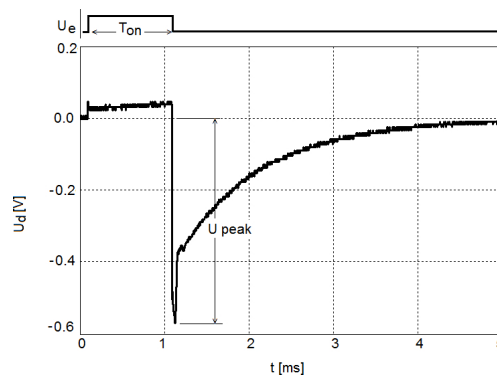


Fig. 2 – Top trace: Waveform of the excitation voltage  $U_e$ . Bottom trace: Waveform of a high voltage pulse recorded by a digital oscilloscope connected to point D.  $U_{peak} \approx -0.57V$  corresponds to output pulse voltage peak value  $\approx -3.88kV$ . Experimental conditions:  $U_{dc}=0$  (no plasma)  $U_g=2V$ ,  $f=100Hz$ ,  $T_{on}=1ms$ .

61 In order to test HVPG operation a plasma source consisting of a cylindrical  
 62 tube made of brass, electrical connected to ground (with role of anode), has been  
 63 used (Fig. 3). The cathode K is a iron wire passing along the longitudinal axis  
 64 of the cylindrical tube. The main characteristic dimensions of the plasma source  
 65 are: cathode diameter  $d = 2$  mm, brass tube inner diameter  $D = 7$  mm, output hole  
 66 diameter  $a = 2$  mm. As a carrier gas was used Ar. The gas flow expels plasma  
 67 through the output hole of the cylindrical tube forming a plume about 2-6 mm in  
 68 length, as a function of experimental conditions.

69 A PIN photodiode Hamamatsu S5972 [18], PD, with maximum sensitivity at  
 70 800 nm, placed near the plasma source output hole, is directed normal to the plasma  
 71 plume ejection direction. Its role is to monitor infrared optical emission of the plasma  
 72 plume. The photodiode PD electrical signal is amplified and filtered, the resulting  
 73 voltage  $U_{pd}$  representing a measure of the plasma plume state. Because infrared opti-  
 74 cal emission exhibits fluctuations in time, the  $R_f C_f$  circuit (time constant  $\tau_f \simeq 0.4s$ ),  
 75 acting as a low pass filter, was inserted at the output of the photodiode amplifier  
 76 (PDA). The whole setup is controlled by a personal computer PC. For this purpose

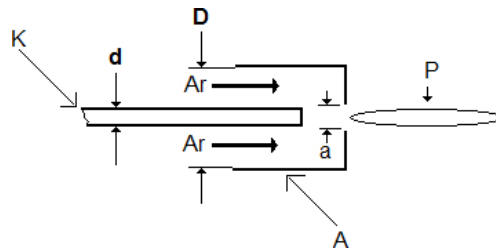


Fig. 3 – Schematic drawing of the plasma source mechanical layout (not in scale). A-anode; K-cathode; P-plasma plume.

77 a specific software application has been developed. The frequency  $f$  and excitation  
 78 voltage  $U_e$  on/off switching is controlled by means of LFG which has a USB con-  
 79 nection with the PC. The analog-to-digital conversion of voltages  $U_1$ ,  $U_2$  and  $U_{pd}$  are  
 80 performed by a general purpose acquisition board (GPAB). An adapter circuits AC  
 81 consisting of voltage dividers and inverter amplifiers converts  $U_1$  and  $U_2$  voltages  
 82 lying in the range -100V to -1000V into the  $U_{d1}$  and  $U_{d2}$  voltages lying in the range  
 83 0.49V to 4.9V, admissible to be applied to the GPAB inputs. Current discharge  $I_{dc}$  is  
 84 calculated by the software application as:  $I_{dc} = |U_2 - U_1|/R_b$ .

### 3. EXPERIMENTAL RESULTS

85 The effect of the high voltage pulses on the plasma plume state, after that is  
 86 initiated, has been investigated. To monitor plasma plume state two parameters have  
 87 been considered:

- 88 -dc current  $I_{dc}$
  - 89 -infrared optical emission of the plasma plume expressed by  $U_{pd}$ .
- 90 Time variation of the  $I_{dc}$  (discharge current) and  $U_{pd}$  if high voltage pulses are  
 91 switched on/off has been recorded. The two graphs correspond to  $|U_{dc}| \approx 495V$   
 92 (Fig.4 ) and  $|U_{dc}| \approx 590V$  (Fig.5), respectively. If applied dc voltage ( $U_{dc} = U_1$ ) is  
 93 lower than a threshold value (Fig. 4 ), it can be seen that plasma plume optical emis-  
 94 sion follows the existence of the high voltage pulses train. When high voltage pulses  
 95 are interrupted, plasma plume vanishes. If applied dc voltage is greater than the  
 96 threshold value (Fig.5 ), a stable plasma plume continues to exist for at least several  
 97 tens of seconds. Note that discharge current  $I_{dc}$  does not describe accurate plasma  
 98 plume state. In Fig.4 spike of the discharge current (denoted by CS) can be observed  
 99 in the absence of plasma. Its existence is due to parasitic discharges occurring in-  
 100 side plasma source. For given electrodes geometry and experimental conditions, the  
 101 lower value of the dc voltage, observed experimentally, for which plasma plume is  
 102 still stable after the high voltage pulses cease, is about 530V.

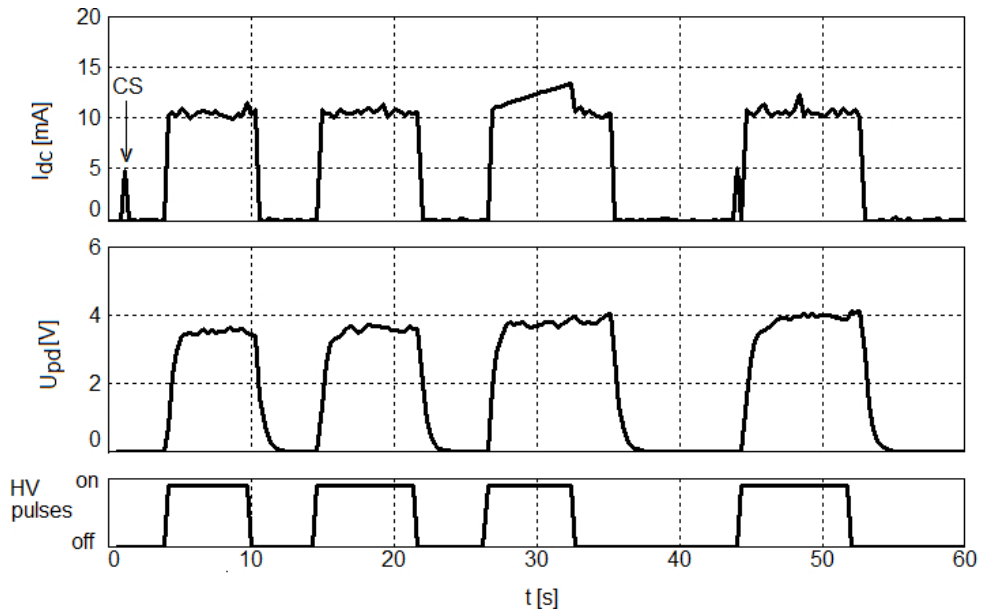


Fig. 4 – Time variation of  $I_{dc}$  and  $U_{pd}$ , if  $|U_{dc}| \approx 495V$ . Experimental conditions:  $R_b = 3k\Omega$ ,  $f=100Hz$ ,  $T_{on}=1ms$ ,  $U_g=3.5V$ .

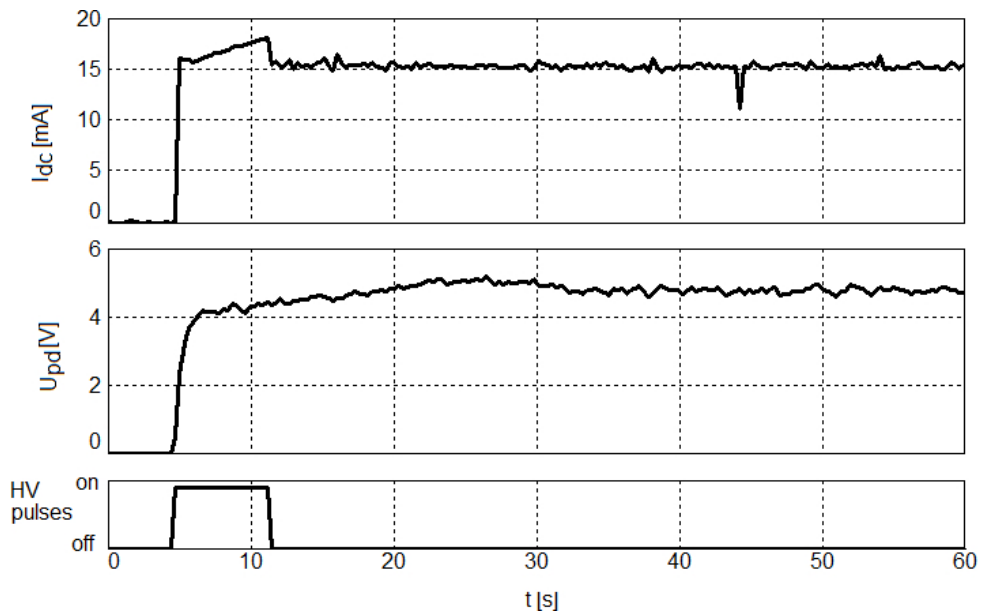


Fig. 5 – Time variation of  $I_{dc}$  and  $U_{pd}$ , if  $|U_{dc}| \approx 590V$ . Experimental conditions:  $R_b = 3k\Omega$ ,  $f=100Hz$ ,  $T_{on}=1ms$ ,  $U_g=3.5V$ .

#### 4. DISCUSSION AND CONCLUSIONS

103 According to the experimental results, after the plasma plume is initiated, for  
104 dc voltage greater than a certain value the electrical discharge continues after the  
105 high voltages pulses are interrupted. The plasma plume state was observed simulta-  
106 neously, optically, by measuring infrared optical emission, and electrically, by calcu-  
107 lating the discharge current, respectively. Electrical method is simpler to implement.  
108 No additionally mechanical accessories are necessary. However this method is prone  
109 to the errors. In some cases, parasitic discharges occurs inside plasma source, so that  
110 a significant  $I_{dc}$  could exist in absence of an external plasma plume. Optical method  
111 is more accurate. Instead, the complexity of the plasma generator, both electrically  
112 and mechanically, increases. The two methods can be combined, to detect operating  
113 anomalies or electrical failures (shortcuts) of the plasma generator. Based on these  
114 observations, as a further work, a procedure aimed to optimize the operation of the  
115 high voltage pulse generator can be devised. If plasma plume is in a normal state,  
116 meaning that its optical emission is above a threshold value, then high voltage pulses  
117 train is switched off. If plasma plume tends to vanish then high voltage pulses train  
118 is switched on.

119 *Acknowledgments.* This work is supported by ANCSI project PN 16 47 01 03-LAPLAS IV

#### REFERENCES

- 120 1. H. Conrads, M. Schmidt, Plasma Sources Sci. Technol. **9**, 441-454 (2000)
- 121 2. A. Bogaerts, E. Neyts, R. Gijbels, J. van der Mullen, Spectrochimica Acta Part **B 57**, 609-658  
122 (2002)
- 123 3. T. Shimizu et al, Plasma Processes and Polymers, **5**, 577-582 (2008)
- 124 4. G. Fridman, G. Friedman, A. Gutsol, A. B. Shekhter, V. N. Vasilets, A. Fridman, Plasma Process.  
125 Polym. **5**, 503-533 (2008)
- 126 5. K. Fricke et al, Plos One, 7, No. 8, e42539 (2012)
- 127 6. A. L. Mihai, D. Dobrin, M. Măgureanu, M. E. Popa, Romanian Reports in Physics, **66**, No. 4,  
128 1110-1117 (2014)
- 129 7. O. V. Penkov, M. Khadem, W-S. Lim, D-E. Kim, J. Coat. Technol. Res., 12 (2) 225-235 (2015)
- 130 8. O.S.Stoican, European Physical Journal-Applied Physics, **55**, 30801 (2011).
- 131 9. A. I. Al-Shamma'a, S. R. Wylie, J. Lucas, C. F. Pau, J. Phys. D: Appl. Phys. **34** 2734-2741 (2001)
- 132 10. N. Georgescu, C. P. Lungu, A. Lupu, Romanian Reports in Physics, vol. 62, No. 1, 142-151 (2010)
- 133 11. S. D. Anghel, A. Simon, M. A. Papiu, O. E. Dinu, Rom. Journ. Phys., Vol. 56, Supplement, pp.  
134 90-94 (2011)
- 135 12. J. Asenjo, J. Mora, A.Vargas, L.Brenes, R Montiel, J. Arrieta, V.I. Vargas, Journal of Physics:  
136 Conference Series **591**, 012049 (2015)
- 137 13. J. Pawlat, P. Terebun, M. Kwiatkowski, J. Diatczyk, J. Phys. D: Appl. Phys. **49**, 374001 (2016)
- 138 14. A. Schütze, J. Y. Jeong, S. E. Babayan, J. Park, G. S. Selwyn, R. F. Hicks, IEEE Transactions on  
139 Plasma Science, **26**, No. 6, 1685-1694 (1998)

- 140 15. L. Wuidart, Topology for switched mode power supplies, Application Note 513/0393, ST Micro-  
141 electronics, 1999
- 142 16. M. Kamil, Switch Mode Power Supply (SMPS) Topologies (Part I), Application Note AN1114,  
143 Microchip Technology Inc, 2007
- 144 17. Vishay Siliconix, IRF840, SiHF840 Datasheet, Doc. No. 91070, S16-0754-Rev.D, 02-May-16
- 145 18. Hamamatsu Photonics, Si PIN photodiode, S5971, 5972, 5973 series